

**OMAE2009-80034**

**A ROBUST AND EFFICIENT COMPUTATIONAL METHOD FOR FATIGUE  
RELIABILITY UPDATE USING INSPECTED DATA**

**Y-T. (Justin) Wu**

Applied Research Associates, Inc.  
Raleigh, NC, USA

**A. P. Ku**

Ergo Engineering, Inc.  
Houston, TX, USA

**C. M. Serratella**

American Bureau of Shipping  
Houston, TX, USA

**ABSTRACT**

This paper presents a new methodology for reliability-based inspection planning focusing on robust and accurate computational strategies for fatigue-reliability updating using inspection results. The core of the proposed strategy is a conditioned sampling-based method, implemented by a Fast Probability Analyzer (FPA) software where efficiency is achieved by using the importance sampling principal. For a single component or limit state, FPA first generates Markov-Chain Monte Carlo (MCMC) samples in the failure domain, then applies an adaptive stratified importance sampling (ASIS) method to compute probability of failure (PoF) with error control. Once the MCMC samples have been created, solving a reliability updating problem is fairly straightforward and computationally robust relative to the conventional system reliability methods that rely on linearization of the limit states. The new approach is demonstrated using examples including stiffened panels of a ship-shaped vessel where reliability is updated using inspection results from 100 panel connections.

**1. INTRODUCTION**

The potential benefits of risk-informed inspections include improved reliability, reduced accidents or incidents that cause safety, environmental, and economics consequences, life extension, and re-qualification (Ref. 1). However, uncertainties, especially systematic uncertainties due to modeling errors/bias and unknowns, may force analysts to apply a large safety factor to the risk estimate and

significantly reduce the usability of risk-based decision making. In many engineering applications, the Bayesian-update methodology has been widely used for uncertainty reductions by using a collection of evidence/observations, including loading/usage histories and observations from inspections. The approach can be viewed as a reverse-engineering tool to narrow down the causes that can explain the observed evidence.

Bayesian reliability updating using inspection data can help design cost-optimal maintenance plans while helping safeguard integrity by inspecting at optimal times when the cracking or corrosion defects can be reasonably detected and fixed if it is determined that they could lead to a failure during the service life. This paper will describe a general risk-based maintenance optimization methodology, and will focus on one aspect of maintenance optimization, i.e., minimizing the number of inspections needed (in one or more vessels) in order to gather enough evidence to help conclude that the updated reliability has achieved a certain target reliability level. For ship structures, the number of inspected locations can be very large ( $> 100$ ). To simplify the problem, but without losing generality, this paper will solve an example with up to 100 inspected connections that experienced similar stresses.

Due to the difficulties in formulating computationally tractable approaches for large numbers of components, most

existing calculation procedures focus on individual components and consider system effects in a simplified, or even crude and error-prone, manner. Several approximation approaches such as the first-order reliability method (FORM) solve a system problem by using linearized limit states, with approximate correlations, in the transformed standard normal space (Ref. 2-4). For reliability updates involving a large number of components, it is computationally difficult and, furthermore, practically impossible to assess the errors introduced by linearizations. Even though several bounding solutions have been proposed, they typically consider up to second-order joint probabilities and also must rely on correlation approximations (Ref. 5). To overcome the numerical and accuracy issues, standard Monte Carlo method can be used, but the computational burden can be overwhelming for typical high reliability (small PoF) problems. This paper will describe a more efficient sampling method without using approximate limit states. While the proposed approach is not as efficient as the ones using linearized limit states, it is numerically robust to handle problems with a large number of limit states or inspections and, as demonstrated in selected examples, it provides a good degree of PoF error-control.

Reliability update can be achieved in at least three ways (Refs. 5-6): through inspection events, through variables, and through regression analysis and adjustment. The focus of this paper is to develop and apply the importance-sampling based approach to update reliability through inspection events, especially for problems with a large number of inspection locations.

## 2. NOMENCLATURE

AIS: Adaptive Importance Sampling  
 ASIS: Adaptive Stratified Importance Sampling  
 FORM: First Order Reliability Method  
 FPA: Fast Probability Analyzer  
 JPDF: Joint PDF  
 MCMC: Markov Chain Monte Carlo  
 MPP: Most Probable Point in the standard normal space  
 RV: Random Variables  
 $\beta$ : Minimum distance  
 $p_f$ : Probability of failure  
 $p_f^o$ : Probability of failure without inspections  
 $\Phi(\cdot)$ : CDF of standard normal  
 $\phi(\cdot)$ : PDF of standard normal  
 $u$ : Standard normal variate

## 3. COMMONLY USED RELIABILITY METHODS

To illustrate reliability methods, fatigue fracture is used as the failure criterion. Under cyclic loading, a small defect caused by, e.g., corrosion (after a coating failure) may grow and result in a fracture failure when the stress-intensity factor  $K$  reaches the fracture toughness  $K_c$ . The fracture limit state is:

$$K(X_1, \dots, X_n, N_s) = K_c \quad (1)$$

The stress-intensity factor is a function of service life,  $N_s$ , and the random variable vector  $\mathbf{X}$  that includes all but the inspection-related random parameters. Alternatively, the limit state can be expressed as:

$$g(\mathbf{X}, N_s) = N_f(\mathbf{X}) - N_s \quad (2)$$

where  $N_f$  is cycles-to-failure. The PoF without inspection, denoted as  $p_f^o$ , can be formulated using an integral as:

$$p_f^o = \Pr.[N_f(\mathbf{X}) \leq N_s] = \int_{N_f \leq N_s} \dots \int f_{\mathbf{X}}(\mathbf{X}) d\mathbf{X} \quad (3)$$

in which  $f_{\mathbf{X}}(\mathbf{X})$  is the joint PDF of  $\mathbf{X}$ . Many structural reliability methods can be used to estimate  $p_f^o$  (Refs. 3-6). Relative to the “with-inspection” case, this integral is easier to compute since many approximation methods may be suitable.

### 3.1 MPP-Based Methods

For well-behaved functions, some of the more widely used approximation methods include First-Order Reliability Method and Second-Order Reliability Method (Refs. 2-4, 6-9), which are based on Taylor’s expansion at the Most Probable Point, MPP, in the transformed space of standard normal variables,  $\mathbf{u}$ .

Denoting the original CDF of  $\mathbf{X}$  as  $F_{\mathbf{X}}(\mathbf{x})$  and the standard normal CDF of  $\mathbf{u}$  as  $\Phi(\mathbf{u})$ , the transformation between  $\mathbf{X}$  and  $\mathbf{u}$  is done by using  $x_i = F_{X_i}^{-1}(\Phi(u_i))$  for independent random variables and by Rosenblatt and other transformations for correlated random variables (Ref. 2). In the  $\mathbf{u}$ -space, it is more convenient to estimate the probability using simple approximate g-functions. In the independent Gaussian space, Eq. 3 becomes:

$$p_f^o = \Pr.[N_f(\mathbf{X}) \leq N_s] = \int_{N_f \leq N_s} \dots \int \phi_{\mathbf{u}}(\mathbf{u}) d\mathbf{u} \quad (4)$$

in which  $\phi_{\mathbf{u}}(\mathbf{u})$  is the standardized-normal JPDF. Figure 1 shows the JPDF of a bivariate Gaussian distribution after removing the JPDF from the failure region that represents the density volume of  $p_f$ . If the g-function is well-behaved, the  $p_f$  volume may be well-represented by a volume-cut centered at the maximum JPDF point, or MPP (also called Design Point or Minimum Distance Point). The MPP-based approximation may provide fast analysis but is known to

perform poorly for “ill-behaved” failure surfaces such as a non-smooth failure surface or a surface with multiple MPPs.

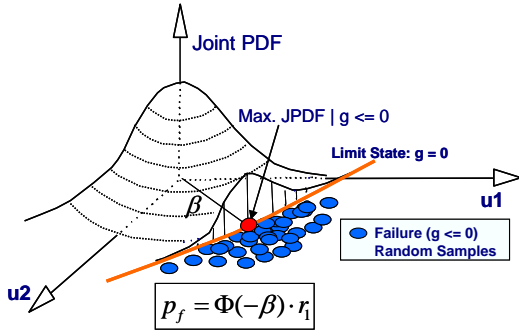


**Figure 1. MPP-Based Method for Computing  $p_f$**

The MPP-based results can be represented as:

$$p_f^o = \Phi(-\beta) \cdot r_1 \quad (5)$$

in which  $\beta$  is the distance from the origin to the MPP, and  $r_1$  is an error factor. The FORM solution assumes  $r_1 = 1$ . The SORM solution also involves the curvature at the MPP.

For system reliability problems, the MPPs from the components can be used to develop simplified approximations using linear limit states. For example, for a series system, in which the failure of any of the  $n$ -components will result in a system failure, the system PoF can be approximated as (Ref. 5):

$$p_{f,sys} = P\left[\bigcup_{i=1}^m (g_i(t) \leq 0)\right] \approx 1 - \Phi_n(\bar{\beta}, \bar{\rho}) \quad (6)$$

in which  $\Phi_n(\cdot)$  is the  $n$ -variate standard normal distribution function,  $\bar{\beta} = (\beta_1, \beta_2, \dots, \beta_n)$  is the  $\beta$ -vector, and  $\bar{\rho}$  is the correlation matrix which is estimated using linear limit states. The accuracy of Eq. 6 depends not only on how well the original limit states can be approximated by linear limit states, but also on the quality of  $\bar{\rho}$ . For more complex systems with a combination of serial and parallel sub-systems, further approximations will be required. Consequently, the resulting errors cannot be assessed using other methods such as Monte Carlo.

#### 4. IMPORTANCE SAMPLING METHDOLOGY

The methodology proposed in this paper is based on the importance sampling concept that generates samples in a targeted domain, in the random variable space, by using a strategically selected JPDP in order to more efficiently generate samples in the region of importance.

#### 4.1 Two-Stage Sampling Framework

The proposed importance sampling strategy is built on the two-stage sampling framework illustrated in Figure 2 (Refs. 10-13). The objective of Stage 1 is to efficiently generate random samples from the failure (or, more generally, conditioned) region, without any maintenance. The resulting PoF can be viewed as the upper bound since the risk can be reduced only by inspecting in time to fix (repair or replace) defected structures before they fail. In Stage 2, only the conditioned/failure samples are re-assessed assuming various maintenance strategies for risk-based optimization.

The standard Monte Carlo simulation procedure can be applied to generate un-conditioned (both safe and failure) samples first and then to generate conditioned samples by filtering; unfortunately, such a process is known to be very time-consuming for structural reliability. In the following sections, several existing methods will be reviewed first, followed by the more recent MCMC-based method.

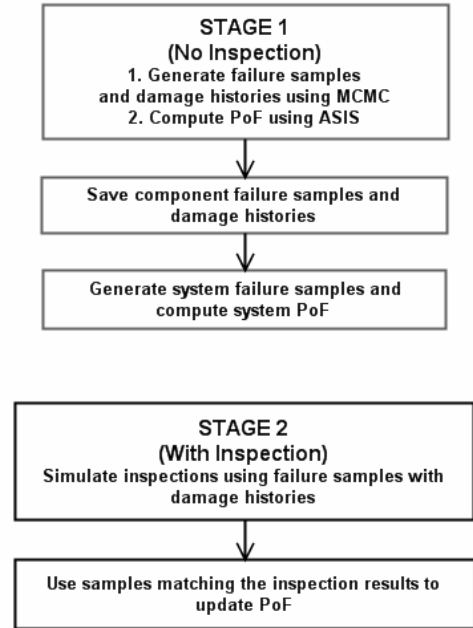


**Figure 2. Two-Stage Sampling Framework**

Assuming the Stage 1 failure samples have been generated, the PoF with inspections,  $p_f^w$ , can be computed as:

$$p_f^w = p_f^c \cdot p_f^o = \frac{\text{No. of failures with insp.}}{\text{No. of failures without insp.}} \cdot p_f^o \quad (7)$$

In which  $p_f^c$  is the PoF, with inspection, conditioned on the Stage 1 failure samples.

## 4.2 Stage-1 Sample Generators

### 4.2.1 Existing Importance Sampling Methods

Several methods exist to generate Stage 1 samples. Earlier methods include the Adaptive Importance Sampling approach (AIS, Ref. 13) which generates samples in the failure region using a parabolic failure surface with adaptively increased curvatures at the MPP. It has been demonstrated that, for well-behaved functions, AIS can improve on the MPP-based results. However, the performance of the method is sensitive to the accuracy of MPP. A more recent method, which is less sensitive to the actual location of MPP, is based on using a conservative limit state (Refs. 11-12). This approach consists of four steps:

Step 1. Find the MPP and estimate PoF using  $p_f^o = \Phi(-\beta)$ .

Step 2. Conduct a second FORM analysis using an adjusted limit state defined as:

$$g(\mathbf{X}, N_s) = N_f(\mathbf{X}) - A \cdot N_s \quad (8)$$

where  $A \gg 1$  is a "safety factor" to generate conservative samples in Step 3 to check the solution from Step 1. Ideally, the adjusted failure region should approximately contain the true failure region ( $p_f^A \gg p_f^o$ ).  $A$  can be selected based on  $p_f^o$  to anticipate a  $p_f^A$  that is, say, 30% larger, by parallel-shifting the MPP tangent surface to reduce  $\beta$ . To speed up Step 2, the first MPP is used as the initial guess to search for the second MPP.

Step 3. Generate samples directly in the adjusted ( $g < 0$ ) region using the second MPP. The generated samples will in general include failures as well as safe samples, as illustrated in Figure 3.

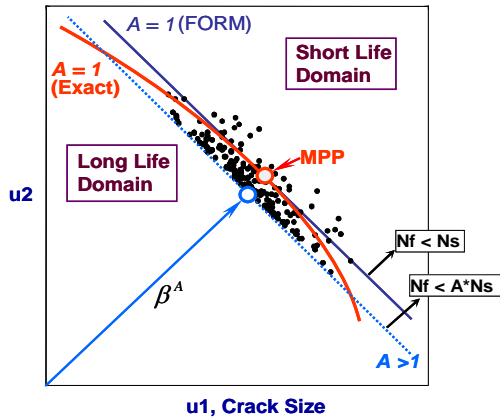


**Figure 3. Generate Stage-1 Failure Samples and Compute  $p_f^o$  using a Conservative Limit State**

Step 4. Re-compute  $p_f^o$  using the samples from Step 3:

$$p_f^o = \Phi(-\beta^A) \cdot \frac{\text{No. of failures without inspections}}{\text{Total number of samples}} \quad (9)$$

in which the number of failures without inspections is based on the Step-3 samples. If the updated  $p_f^o$  is significantly different, that would suggest using a larger  $A$  and more samples. If results do not converge after using more conservative  $A$  values, other methods should be used.

Step 5. Compute the PoF with inspections,  $p_f^w$ , as:

$$p_f^w = p_f^c \cdot p_f^A = \frac{\text{No. of failures with insp.}}{\text{No. of failures without insp.}} \cdot p_f^A \quad (10)$$

### 4.2.2 Markov-Chain Monte Carlo (MCMC)

MCMC can be used to generate failure or conditioned samples by reducing the JPDF to zero in the safe region, and to generate samples in the failure domain according to the original JPDF in the failure region, without the need to compute the scaling factor to create a valid joint PDF in the failure region. Figure 4 illustrates that, once a seed sample has been found in the failure region after an initial exploration search, the subsequent MCMC sampling can stay within the failure domain and generate samples according to the JPDF. With the proper selection of a "proposal distribution" for a random walk, the samples will converge to the targeted distribution in the failure region. One of the well-known MCMC sample-generation methods is the Metropolis-Hastings algorithm that was implemented in the FPA software to generate 1-2 thousand MCMC samples. For more information on the MCMC method, see (Refs. 14-15).

The MH algorithm can be summarized as follows:

- (1). Explore the space to find a starting point in  $g < 0$ .
- (2). A proposal distribution,  $q(\mathbf{x}_{New} | \mathbf{x}_{Current})$ , is selected to generate a random move to a candidate point  $\mathbf{x}_{New}$ .
- (3). Compute  $f(\mathbf{x}_{New})$ ,  $f(\mathbf{x}_{Current})$ ,  $q(\mathbf{x}_{Current} | \mathbf{x}_{New})$ , and  $q(\mathbf{x}_{New} | \mathbf{x}_{Current})$ .
- (4). Compute  $g(\mathbf{x}_{New})$  and let  $f(\mathbf{x}_{New}) = 0$  if  $g(\mathbf{x}_{New}) > 0$ .
- (5). Accept the new point with a probability of

$$\rho = \min \left[ \frac{f(\mathbf{x}_{New})}{f(\mathbf{x}_{Current})} \cdot \frac{q(\mathbf{x}_{Current} | \mathbf{x}_{New})}{q(\mathbf{x}_{New} | \mathbf{x}_{Current})}, 1 \right].$$

- (6). Reject the candidate point and save the current point as the "next" point with a probability of  $1 - \rho$ .

The above Step 4 ensures that candidate points in the safe domain will be rejected with a probability of one; consequently, all the generated points will be in the failure domain. Steps 5 and 6 can be executed using a uniform random number generator.

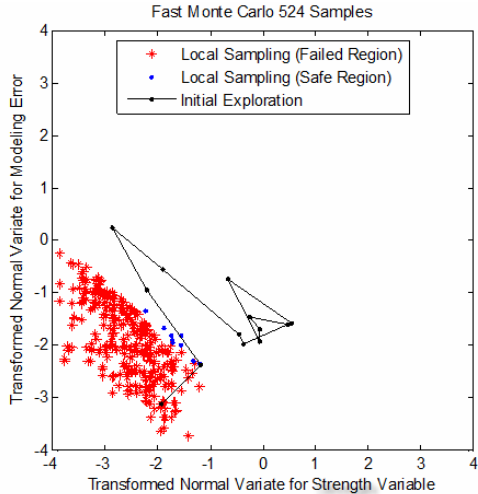


**Figure 4. MCMC with 500 Failure Samples**

The selection of the proposal distribution will affect the acceptance/rejection rate. In this work, a simple uniform distribution that centers at the current point and with a tuned range has been chosen. Since the distribution is symmetrical,  $q(x_{Current} | x_{New}) / q(x_{New} | x_{Current}) = 1$ ; as a result, the ratio of the PDFs of the current and candidate points drives the random movement in a way that ensures that the frequency of visits at any point will be asymptotically proportional to the JPDF in the failure region. The range of the uniform distribution defines the maximum step size of each random move and can significantly affect the rejection rate and the convergence rate towards the target distribution, and therefore needs to be tuned. A burn-in period (in which the samples would be thrown away) of several hundred samples is usually needed to help avoid initial outliers. For high (> 5) dimension problems, the acceptance rate will decrease drastically and slow down the converging process. To address the issue, a modified M-H algorithm may be used (Ref. 16).

Unlike MC, the sequence of MCMC samples is not independent and the convergence to the target PDF may be slower; therefore, the quality of the randomness is inferior to MC and should be used with caution. MCMC may be more difficult to implement, but, if done properly, it is more robust because of its ability to handle non-smooth failure surfaces.

#### 4.2.3 Adaptive Stratified Importance Sampling

The MCMC samples do not provide the probability of failure itself but can be used as pilot samples to support importance-sampling probabilistic analysis. ASIS uses MCMC samples to envelop the failure region. Provided that MCMC is successful (i.e., samples are correctly distributed in the failure regions), ASIS can control the sampling error within the MCMC-covered failure region. A more detailed summary of ASIS is included in Annex A.

### 4.3 Sampling Based System PoF Analysis

To extend the component reliability approach to system reliability problems, the MCMC-based failure samples are generated for each component first, and then a bootstrap procedure is applied to draw samples according to component PoFs to create non-redundant system failure samples and estimate system PoF. The system PoF is estimated by building system samples one by one, from the components, proportional to the PoFs. Starting from the top-ranked component, each added sample is checked for multiple events, and the sample is removed if it causes a redundant failure.

For a reliability updating problem, the focus is on the samples that match the inspected results. In other words, the updated failure is conditioned on those samples, e.g., missed detections.

## 5. FATIGUE RELIABILITY EXAMPLE

### 5.1 Single Connection

This example is based on a tanker panel connection example (Ref. 17). Assuming a surface crack in a connection, the limit-state function can be written as (Ref. 18):

$$M(t) = \int_{a_o}^{a_f} \frac{da}{(\varepsilon_Y Y(a) \sqrt{\pi a})^m} - C v T \varepsilon_s^m A^m \Gamma\left(1 + \frac{m}{B}\right) \quad (11)$$

where

- $a_o$  = Initial crack depth
- $a_f$  = Final crack depth at failure
- $Y(a)$  = Geometry function of the crack shape
- $C, m$  = Crack growth parameters
- $v$  = Stress range annual frequency (cycles/year)
- $T$  = Time under consideration (year)
- $\varepsilon_Y$  = Model uncertainty for geometry function
- $A, B$  = Weibull parameters for stress range

The RVs and fixed parameters are summarized in Table 1.

**Table 1. Input Data for Fatigue Example**

Random Variables					
X	Name	Description	Distribution	Para. 1	Para. 2
X(1)	a <sub>i</sub>	Initial crack depth (mm)	Exponential	0.11	0.11
X(2)	c	Crack growth parameter (lnC)	Normal	-29.7	0.29997
X(3)	ln_A	Weibull stress parameter (lnA)	Normal	2.26	0.14916
X(4)	Inv_B	Weibull stress parameter (1/B)	Normal	1.43	0.1001
X(5)	es	Stress modeling error	Normal	1	0.1
X(6)	ey	Random geometry factor	Normal	1	0.1
X(7)	a <sub>D</sub>	MPI detectable crack length (mm)	Exponential	0.1279	0.1279
Deterministic Variables					
DX	Name	Description	Values		
DX(1)	v <sub>o</sub>	Average stress cycles per year	2.50E+06		
DX(2)	m	Crack growth parameter	3		
DX(3)	r	Crack aspect ratio (a over C)	0.15		
DX(4)	z	Plate thickness (mm)	30		
DX(5)	b	Plate width (mm)	10000		
DX(6)	T	Time (years)	5		
DX(7)	a <sub>f</sub>	Final crack depth (mm)	30		
DX(8)	a <sub>m</sub>	Measured crack depth (mm)	10		

The inspection limit-state function is:

$$I_{no}(t) = \int_{a_o}^{a_D} \frac{da}{(\varepsilon_Y Y(a) \sqrt{\pi a})^m} - CvT \varepsilon_S^m A^m \Gamma\left(1 + \frac{m}{B}\right) \quad (12)$$

where  $a_D$  is the detectable crack depth which is typically a random variable associated with the probability of detection (POD). The POD used for the example has an exponential distribution with  $\lambda = 0.1279 \text{ mm}^{-1}$ :

$$POD(a) = 1 - \exp(-\lambda a) \quad (13)$$

The probability formulation for reliability update with no crack found is:

$$p_f = P[M(t) < 0 | I_{no}(t_{inspect}) > 0] \quad (14)$$

In the previous study, Eq. 14 was analyzed using the FORM method. In this paper, the following limit-state function is used for generating fail or safe MCMC samples and the samples are used for Bayesian updating.

$$g = T - t_{service} = \frac{\int_{a_o}^{a_f} \frac{da}{(\varepsilon_Y Y(a) \sqrt{\pi a})^m}}{Cv \varepsilon_S^m A^m \Gamma\left(1 + \frac{m}{B}\right)} - t_{service} \quad (15)$$

Assuming  $m = 3$ , and  $Y(a) \approx 1.12$ , the above equation can be simplified as:

$$g = T - t_{service} = \frac{\frac{2}{\varepsilon_Y^3 (1.12)^3 \pi^{1.5}} \left[ \frac{1}{\sqrt{a_o}} - \frac{1}{\sqrt{a_f}} \right]}{Cv \varepsilon_S^3 A^3 \Gamma\left(1 + \frac{3}{B}\right)} - t_{service} \quad (16)$$

For inspection simulation purposes, the crack size at inspection time is needed and can be derived from Eq. 16 as:

$$a(t_{insp}) = \frac{1}{\left[ \frac{1}{\sqrt{a_o}} - \frac{Cv t_{insp} \varepsilon_S^3 A^3 \Gamma\left(1 + \frac{3}{B}\right)}{2 / \varepsilon_Y^3 (1.12)^3 \pi^{1.5}} \right]^2} \quad (17)$$

The POD function in Eq. 13 is applied to the calculated crack size from Eq. 17 to simulate the effect of detection – detected or missed.

### 5.1.1 Reliability Without Inspection

The  $p_f^o$  was calculated using ASIS which took a few seconds on a notebook. The PoF convergence history is shown in Figure 5 which shows a quick convergence. To demonstrate the consistency and accuracy of ASIS, 100 ASIS runs were executed, and the results, shown in Figure 6, demonstrate that the PoF scatters are within +/- 5% error bounds, as targeted.

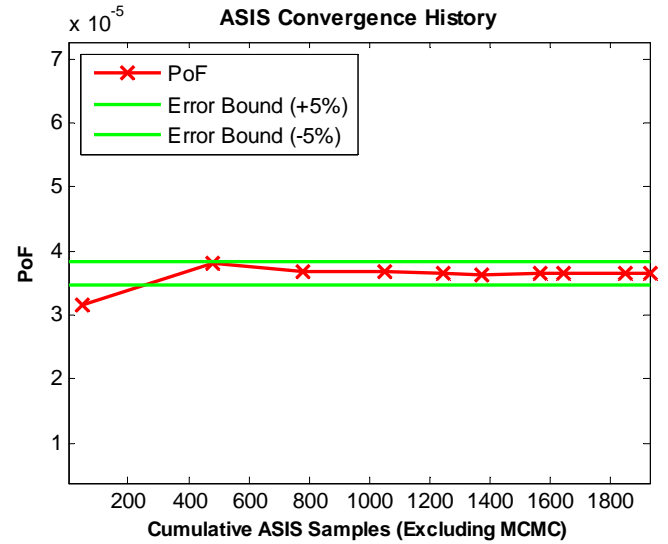


Figure 5. ASIS Convergence History

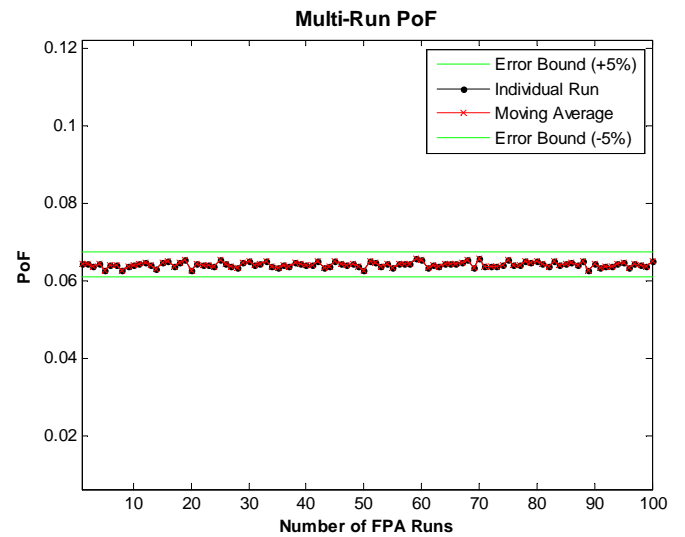
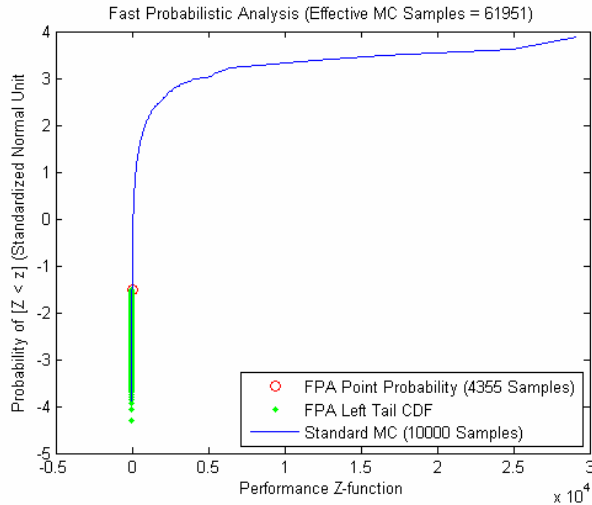


Figure 6. ASIS within 5% Error

Figure 7 shows the CDF plot using 10,000 Monte Carlo samples and 4355 MCMC failure samples. It should be noted that the number of MCMC samples needed is generally independent of  $p_f$ , and therefore is increasingly more

efficient for smaller  $p_f$ , when compared with the MC method. These failure samples are saved for reliability updating analyses. For reliability updating, MC was conducted with 10,000 samples to generate 9355 safe samples. In general, more samples, if affordable, should be used. However, experience suggests that numbers in the order of 1000 are usually sufficient.



**Figure 7. Fatigue Reliability (without inspections)**

The above reliability result was close to the result in the original paper ( $p_{FORM} \approx 0.0668$ ), suggesting that the FORM method is accurate. By varying the service time from 1 to 20 years, the resulting reliability curve is shown in Fig. 8.

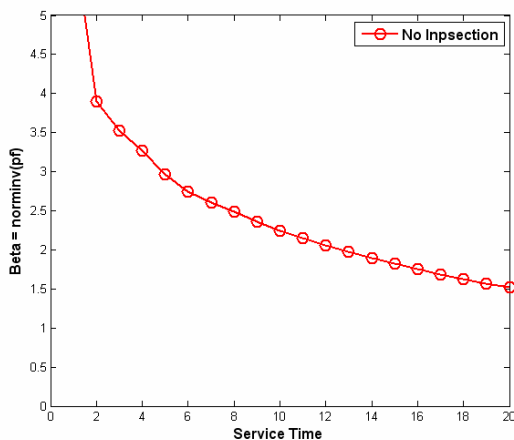


**Figure 8. Fatigue Reliability (without inspections) versus Service Time**

### 5.1.2 Reliability-With-Inspection

The procedure to update reliability-with-inspections using the two-stage procedure is summarized in the following steps:

1. Generate  $K_f$  failure samples using MCMC and compute  $p_f^o$  (base-line PoF).
2. Generate  $K_s$  safe samples using the MC approach.
3. Using crack growth and inspection simulation, track the crack sizes and estimate the ratio of missing the inspection/detection from the safe population,  $r_{S\_Missed}$ .
4. Using crack growth and inspection simulation, track the crack sizes and identify and store the samples from  $K_f$ , denoted as  $K_{f\_Missed}(t_{insp})$ , that have missed the inspection at time of inspection.
5. Using crack growth and inspection simulation, track the crack sizes of all the  $K_{f\_Missed}(t_{insp})$  samples and count the numbers as a function of time,  $K_{f\_Missed}(t)$ .
6. The updated probability of failure can be estimated by:

$$p_f^u = \frac{K_{f\_Missed}(t)}{K_{f\_Missed}(t_{insp}) + K_s \cdot r_{S\_Missed}} \quad (18)$$

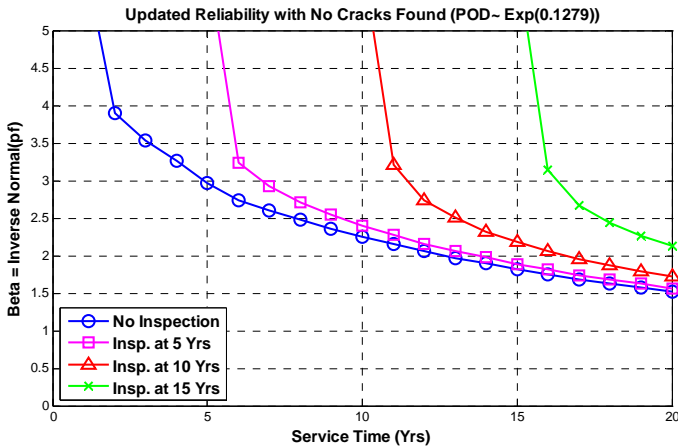
$$= \frac{K_{f\_Missed}(t)}{K_{f\_Missed}(t_{insp}) + K_f \left( \frac{1 - p_f^o}{p_f^o} \right) \cdot r_{S\_Missed}}$$

in which the denominator is the total number of samples that have missed the inspections, and the numerator is the number of failure samples that have missed the inspections.

The safe samples are needed for estimating  $r_{S\_Missed}$  in Eq. 18. In practical applications, the safe samples are typically associated with parts with smaller defect sizes; therefore, the probability of missing a defect from safe samples, i.e.,  $r_{S\_Missed}$ , should be fairly large (say  $> 0.1$ ) relative to  $p_f$ , which means a large number of safe samples is typically not required.

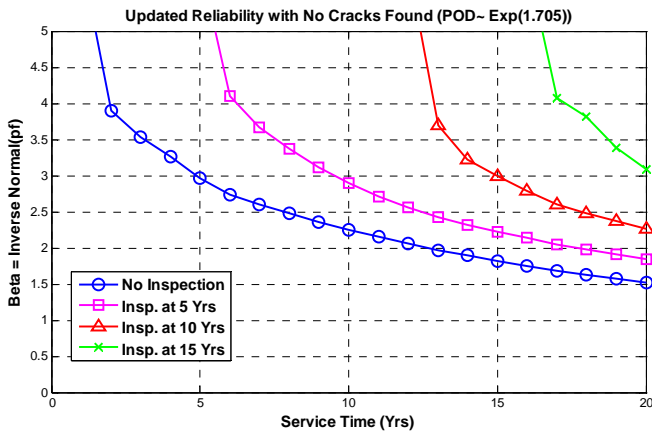
To avoid using the safe samples, the existing two-stage sampling procedure which uses failure samples needs to be modified by generating MCMC samples conditioned on the inspected outcome:  $[g(t) < 0 | \text{Inspection Result}]$ . The generated samples can be used to update the reliability without additional MC simulations and would be computationally more effective.

Figure 9 results from Eq. 18 and shows the increase of reliability given the evidence that no crack was found after one inspection at 5, 10, or 15 years.



**Figure 9 Fatigue Reliability Updating (Case 1: POD with lambda of 0.1279)**

The result compared well with the earlier result (Ref. 17) using a commercial software with the FORM method. The same set of samples could be used for various inspection conditions. For example, Figure 10 shows the result using a better POD with a larger  $\lambda$ . Comparing Figure 9 with Figure 10, the new updated reliabilities were higher, which was consistent with the fact that, with a better detection capability, a defect was more unlikely to be missed, implying that the structural component had a smaller crack size. Another example involved two inspections, first at 5 years, and again at 10 years. The two-inspection reliability result is plotted in Figure 11, showing a saw-tooth shape.



**Figure 10. Fatigue Reliability Updating (Case 2: POD with lambda of 1.705)**

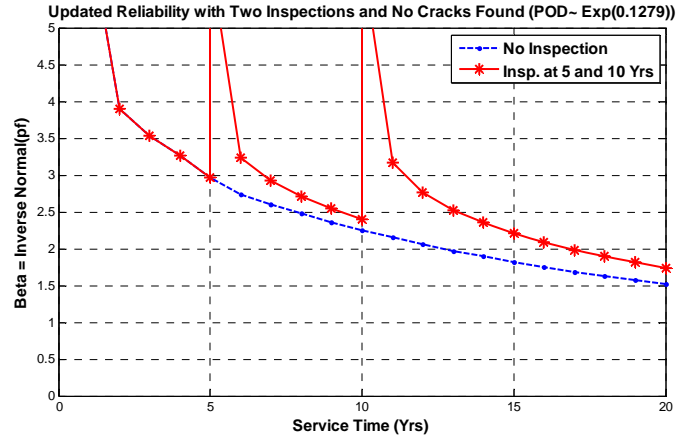


**Figure 11. Fatigue Reliability Updating (Case 3: Two Inspections at 5 and 10 years; POD with lambda of 0.1279)**

### 5.2 Multiple Inspected Connections

In this example, the objective is to update the reliability of an un-inspected connection using the inspected connections. Assuming  $m$  connections have been detected with no cracks, the formulation is:

$$p_f = P[M(t) < 0 | I_1 < 0 \cap I_1 < 0 \cap \dots \cap I_m < 0] \quad (19)$$

Using the sampling approach, the required random samples for the inspected connections were generated by conditioning on the samples of the un-inspected connection. To simplify the illustration example, the random variables A and B, two of the distribution parameters in the Weibull distribution that modeled the long-term stress range, were treated as common (fully dependent) random variables. This simplified model was used to investigate whether or not the sampling-based approach could deal with reliability inference using a large amount of relevant inspection data. It should be noted that in real applications, A and B may be different among the inspected connections; however, they tend to be statistically strongly correlated if the inspected connections experienced similar loading histories. In general, comprehensive correlation models that more closely represent the real loading conditions should be developed and used. The results below demonstrate that the importance sampling-based framework is indeed capable of handling a large number of connections.

The analysis results for up to 100 connections are plotted in Figure 12. Notice that the curve is fairly smooth except for  $m > 50$ . The reason is because it became more unlikely to produce a set of samples that would meet the “all missed” conditions for un-inspected connections. This trend suggests that for larger numbers of connections, more samples are needed to reduce statistical error.

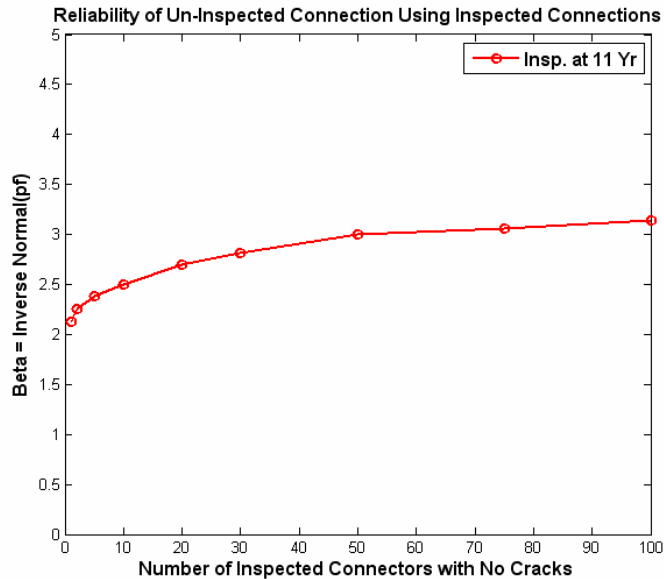


**Figure 12. Fatigue Reliability Updating of Un-inspected Connection using Inspected Connections**

Figure 12 shows that the updated reliability increased with more inspected connections without cracks, but the rate of increase slowed down as the number of connections increased. In fact, the reliability seemed to slowly approach an upper bound. The trend may be explained by the fact that there were independent random variables (see Table 1) and therefore the uncertainty of the un-inspected connection could not be completely eliminated regardless of how many inspected connections were found to have no cracks.

## 5. SUMMARY

This paper presented a computationally efficient and robust two-stage importance sampling methodology for reliability updating using inspection data. By analyzing a problem with 100 inspected connections, we have demonstrated that the approach has these unique strengths: (1) Capable of dealing with large and complex inspection and maintenance planning issues, (2) More robust and accurate than the conventional MPP-based approximate approaches, and (3) More efficient than the conventional one-stage importance sampling method as Stage 1 samples can be repeatedly used in Stage 2 for various inspection and maintenance scenarios.

The statistical correlations of the random variables among the inspected events are keys to accurate reliability updating and are important to the development of risk-based inspection plans. More development work is recommended in order to

build good correlation models and to generate conditioned correlated samples for reliability updating.

## REFERENCES

1. Ayyub, B.M., Akpan, U.O., Rushton, P.A., Koko, T.S., Ross, J., Lua, J. "Risk-Informed Inspection of Marine Vessels," Ship Structures Committee SSC report 338-I, 2002.
2. Ang, A. H.-S, Tang, W.H. 1984. Probability Concepts in Engineering Planning and Design, Volume II; Decision, Risk, and Reliability, New York, John Wiley & Sons.
3. Thoft-Christensen P., Murotsu, Y. 1986. Application of Structural Systems Theory, Springer.
4. Ditlevsen, O., Madsen, H. O. 1996, Structural Reliability Methods, J. Wiley & Sons, New York, 1996, 384 pp.
5. Moan, T. & Song, R., "Implication of Inspection Updating on System Fatigue Reliability of Offshore structures," 17<sup>th</sup> International Conference on Offshore Mechanics and Arctic Engineering, OMAE98-1214.
6. Madsen, H.O., Skjong, R.K., Talin, A.G., Kirkemo, F. 1987. "Probabilistic Fatigue Crack Growth Analysis of Offshore Structures, with Reliability Updating Through Inspection," SNAME, Arlington, VA.
7. Rackwitz, R. 2001. "Reliability Analysis - A Review and Some Perspectives," Structural Safety, Vol. 23, pp. 365–395.
8. Der Kiureghian, A. 2005. "First- and Second-Order Reliability Methods," Chapter 14 in Engineering Design Reliability Handbook, E. Nikolaidis, D. M. Ghiocel and S. Singhal, Edts., CRC Press, Boca Raton, FL.
9. Nikolaidis, E., Ghiocel, D.M., Singhal, S. (Editors). 2005. Engineering Design Reliability Handbook, CRC Press, Boca Raton, FL.
10. Wu, Y-T., "A Reliability-Based Maintenance Optimization Methodology," Chapter 14 in Structural Design Optimization Considering Uncertainties, Taylor and Francis, 2007.
11. Wu, Y-T., Shiao, M., Shin, Y., Stroud, W.J, "Reliability-Based Damage Tolerance Methodology for Rotorcraft Structures," Transactions Journal of Materials and Manufacturing, 2005.
12. Wu, Y-T., Shin, Y. 2005. "Probabilistic Function Evaluation System for Maintenance Optimization," Proceedings of the AIAA 46th SDM Conference.
13. Wu, Y-T., 1994, "Computational Methods for Efficient Structural Reliability and Reliability Sensitivity Analysis," AIAA Journal, Vol. 32, No. 8, pp. 1717–1723.
14. Robert, C.P., Casella, Monte Carlo Statistical Methods, Springer, 2004.
15. Gamerman, D. 1997. Markov Chain Monte Carlo, Chapman & Hall.
16. Au, S.K., Beck, J.L. 2001, "Estimation of small failure probabilities in high dimensions by subset simulation," Probabilistic Engineering Mechanics, Vol. 16, No. 4, pp. 263-277.

17. Ku, A., Serratella, C., Spong, R., Basu, R., Wang, G., and Angevine, D., "Structural Reliability Applications in Developing Risk-Based Inspection Plans for a Floating Production Installation," OMAE 2004-51119, 2004.
18. Cramer, E.H., Schulte-Strauthaus, R., Bea, R.G., "Structural Maintenance Project Vol. 1 Fatigue Damage Evaluation," Ship Structures Committee SSC report 386-I, 1995.
19. Wu, Y-T., Enright, M.P., Millwater, H.R. 2002. "Probabilistic Methods for Design Assessment of Reliability With Inspection," AIAA Journal, Vol. 40, No. 5, pp. 937-946.

## ANNEX A

### ADAPTIVE STRATIFIED IMPORTANCE SAMPLING

ASIS requires dividing the failure region (i.e., the region is stratified) into  $m$  regions, so that

$$p_f = p = \sum_{j=1}^m A_j p_j \quad (A1)$$

where  $A_j$  is the area of region  $j$ . Assuming  $p_j$  can be approximated by binomial distributions, minimizing the sample variance of  $p$  would lead to the following optimal sizing formulas derived originally for an aircraft rotor design application (Ref. 19):

$$K = \left( 100 \frac{-\Phi^{-1}[(1-CL(\%))/2] \sum A_j \sqrt{p_j q_j}}{\gamma p} \right)^2 \quad (A2)$$

$$k_j = K \frac{\Delta A_j \sqrt{p_j q_j}}{\sum \Delta A_j \sqrt{p_j q_j}} \quad (A3)$$

where  $K$  is the total sample size and  $k_j$  is the sample size in region  $j$ . The error control parameter  $\gamma(\%)$  is the target error bound at a confidence level of CL.

The implemented ASIS computational framework can be summarized as follows:

- Step 1. Generate a sufficient number of MCMC samples (2000 is used in this study).
- Step 2. Define a sampling region, e.g., a linear surface, that covers nearly all the MCMC samples.
- Step 3. Divide the sampling region into several regions ( $> 3$  is used) using a design (e.g., equal probabilities). The number of divisions needs to be tuned to achieve optimal efficiency.

Step 4. Using Eq. A3, adaptively increase the samples in regions to update  $p_j$  for PoF convergence.

The ASIS method has been used in this paper for all the component PoF calculations.

### Simple Illustration Example

This test example has a simple limit-state function with  $g = 4 + 0.5u_1^2 - u_2$ , which has two Gaussian RVs and a parabolic failure surface with  $\beta = 4$ .

Two thousand MCMC samples and a target ASIS error bound of 5% were used and the analysis was run 100 times to check the robustness/reliability of ASIS. Using one of the runs, Figure A1 shows the similar failure pattern produced by the MCMC and ASIS failure samples. Figure A2 plots all the ASIS samples including safe and failure samples.

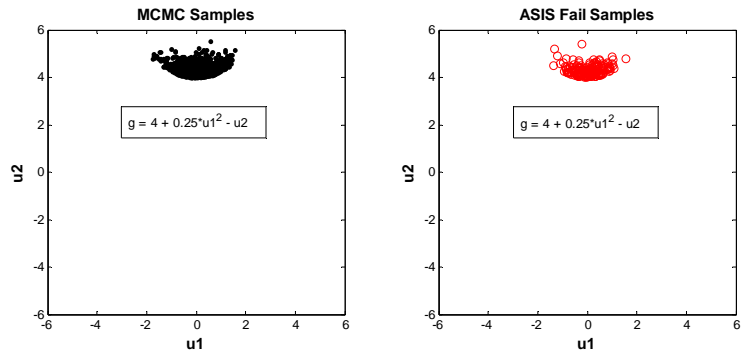


Figure A1. MCMC versus ASIS Failure Samples

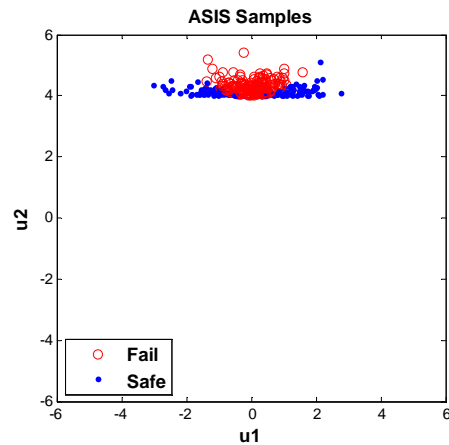
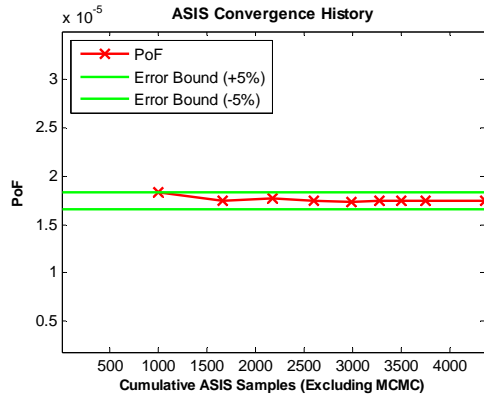


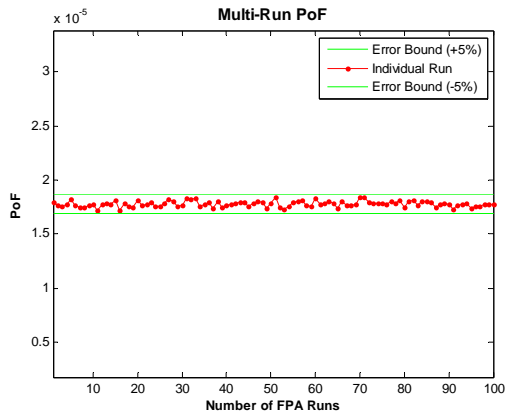
Figure A2. Failure and Safe Samples Generated by the ASIS Procedure

Figure A3 shows a typical ASIS PoF convergence history. On average, about 4000 ASIS samples (not including MCMC samples) were needed to meet the 5% error target. The number reduced to about 1000 for 10% error.



**Figure A3. Example ASIS Convergence History**

The 100-run ASIS results, plotted on Figure A4, were within the target error bound. The average PoF was 1.776e-05.



**Figure A4. 100 ASIS Results All Within +/- 5% Error**

To compare with the MC method, an independent analysis was conducted using 100 MC runs with a sample size of 10 million per run. The analysis produced PoF values ranging from 1.47e-05 to 2.07e-05 with an average of 1.776e-05. Based on the average, the 100 results were within approximately +/-17% error bounds. Using Eq. A2 with  $m = 1$  and 5% error at 99.99% confidence, the required sample size is 341 million, which is about 57000 times the required sample size of the ASIS method.

Using  $\beta = 4$ , the FORM solution is 3.1671e-05 which has an error of 78%. This large error can be explained by the very curved failure surface shown in Figure A2.